

Numerical Investigation of the Nonlinear Penetration of Pulsed Electromagnetic Fields Into a Ferromagnetic Shield with a Simple Exponential Permeability Model

William J. Croisant

U.S. Army Engineer
Research and Development Center Construction Engineering Research Laboratory,
Champaign, IL, USA
w.croisant@ieee.org

Carl A. Feickert

U.S. Army Engineer
Research and Development Center Construction Engineering Research Laboratory,
Champaign, IL, USA
carl.a.feickert@erdc.usace.army.mil

Michael K. McNerney

U.S. Army Engineer
Research and Development Center Construction Engineering Research Laboratory,
Champaign, IL, USA
mkmcinerney@ieee.org

Abstract

Electrically conductive ferromagnetic shielding materials exhibit nonlinear behavior (including magnetic saturation) under intense pulsed electromagnetic field conditions. This paper considers the fundamental problem of a long, thin-walled cylindrical electrically conductive ferromagnetic shield subjected to axially-directed, unipolar, short-duration surface current pulses. A simple idealized relative differential magnetic permeability model is used to portray the nonlinear effects of a field-dependent permeability, including saturation. The transient magnetic field intensity within the shield is investigated using finite difference time domain (FDTD) calculations.

Keywords

Nonlinear, ferromagnetic, permeability, shield, current, transient, pulse, impulse, finite difference time domain.

INTRODUCTION

Electrically conductive ferromagnetic shielding materials exhibit nonlinear behavior (including magnetic saturation) under intense electromagnetic field conditions. The nonlinear behavior under intense transient field conditions is not well understood. This paper considers the fundamental problem of a long, thin-walled cylindrical electrically conductive ferromagnetic shield subjected to axially-directed, unipolar, short-duration current pulses along its exterior surface. In order to facilitate the study of the effects of magnetic parameters on the penetration of the electromagnetic fields, a simple idealized relative differential magnetic permeability model is used to represent the nonlinear effects of a field-dependent permeability, including saturation. Previously, the transient electric field induced at the inner surface by the surface current pulse was considered, and results of mathematical and numerical analyses were presented [1]-[4]. This paper investigates the transient magnetic field intensity within the shield itself. Selected results of finite difference time domain (FDTD) calculations are presented.

DIFFERENTIAL PERMEABILITY MODEL

For ferromagnetic materials, the variation of the magnetic flux density, B , with the magnetic field intensity, H , is described by the magnetization curve, $B(H)$. In this model, the time-dependence of $B(H)$ is not included. It is assumed that B is collinear with H . Hysteresis is neglected, and $B(H)$ is assumed to be a single-valued reversible function of H .

The field-dependent relative differential permeability $\mu_{rd}(H)$ is defined as

$$\mu_{rd}(H) \equiv \frac{1}{\mu_0} \frac{dB(H)}{dH}$$

where $\mu_0 = 4\pi \times 10^{-7}$ henry/meter is the permeability of free space.

A simple magnetization model that exhibits saturation for large values of magnetic field intensity is:

$$B(H) = \mu_0 H + B_s \left[1 - \exp\left(-\frac{H}{H_1}\right) \right]$$

where B_s is the saturation magnetization in teslas and H_1 is a characteristic value in amps/meter. This model is shown in Figure 1.

Magnetization Model

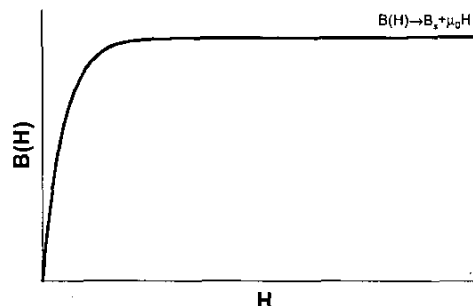


Figure 1. Model for magnetization curve, $B(H)$.
model corresponding to the above magnetization model is:

$$\mu_{rd}(H) = 1 + \mu_{ri} \exp\left(-\frac{H}{H_1}\right)$$

where

$$\mu_{ri} \equiv \frac{B_s}{\mu_0 H_1}$$

This simple differential permeability model is shown in Figure 2.

Differential Permeability Model

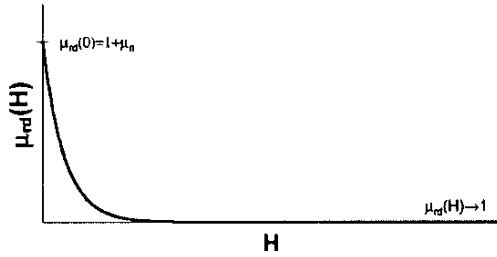


Figure 2. Model for relative differential permeability model, $\mu_{rd}(H)$.

Similar exponential permeability representations have been considered by other authors to model a variety of problems, e.g., [5]-[8]. This simple exponential relative differential permeability model contains two parameters that can be used to model the relative differential permeability, including saturation. The third parameter is constrained by the above relationship. The initial value of the permeability (for $H=0$) is

$$\mu_{rd}(0) = 1 + \mu_{ri}$$

For large values of H , the relative differential permeability approaches unity as the material undergoes saturation

$$\mu_{rd}(H) \rightarrow 1$$

The above differential permeability model does not exhibit all of the details of a physical permeability curve; however, it includes some salient features, and its simplicity facilitates investigations of the role of various parameters.

PROBLEM FORMULATION

The general problem considered in this paper is the transient electric field induced along the inner surface of a long, thin-walled cylindrical electrically conductive ferromagnetic shield subjected to an axially-directed, unipolar,

short duration, surface current pulse along the outer surface. The current pulse leads to a transverse electromagnetic field condition at the outer surface. The problem configuration is shown in Figure 3. This general problem has practical application to cable shields and conduit shields

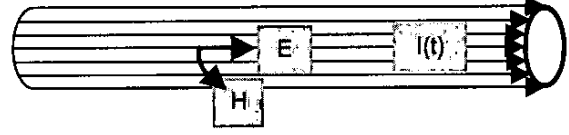


Figure 3. A thin-walled cylinder subjected to an axially-directed surface current pulse.

subjected to short-duration surface current pulses.

For a planar approximation to the thin-walled cylinder problem, a sheet of thickness 'd' and electrical conductivity σ is considered. The magnetic field $H(x,t)$ is described by the nonlinear partial differential equation

$$\frac{\partial^2 H}{\partial x^2} = \sigma \mu_0 \left[1 + \mu_{ri} \exp\left(-\frac{H}{H_1}\right) \right] \frac{\partial H}{\partial t}$$

subject to the initial condition at time $t = 0$

$$H(x,0) = 0;$$

a pulsed surface current condition at the outer surface

$$H(0,t) = A_0 \left[\exp\left(-\frac{t}{t_f}\right) - \exp\left(-\frac{t}{t_r}\right) \right]$$

where A_0 is an amplitude factor (amps/meter), t_r is a time constant associated with the rise-time of the applied pulse, and t_f is a time constant associated with the fall-time of the applied pulse ($t_f > t_r$); and a vanishing field condition at the inner surface

$$H(d,t) = 0$$

since there is no enclosed current in the original problem.

The peak of the applied surface current pulse occurs at

$$t_p = \frac{\ln\left(\frac{t_f}{t_r}\right)}{\frac{1}{t_r} - \frac{1}{t_f}}$$

The applied surface pulse is shown in Figure 4.

Typical Double Exponential Current Pulse at Outer Surface

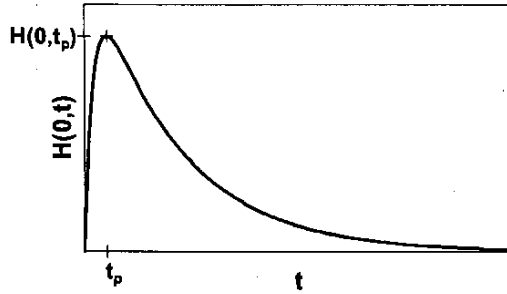


Figure 4. Time variation of typical double exponential applied surface current pulse $H(0,t)$. The peak value of the applied pulse, $H(0,t_p)$ occurs at t_p .

The electric field $E(x,t)$ is determined from $H(x,t)$ by

$$E(x,t) = -\frac{1}{\sigma} \frac{\partial H(x,t)}{\partial x}$$

The electric field transient at the inner surface $E(d,t)$ is of particular interest. Previous work [1]- [4] has shown that the E field at the inner surface will increase with time, pass through a maximum, and then decrease to zero. The peak value of the electric field, E_{peak} , and the time at which the peak value occurs, t_{peak} , are of primary interest. The time variation of a typical electric field transient is shown in Figure 5. For short-duration applied pulses, the peak value of the electric field response occurs significantly later than the peak of the applied surface pulse.

Typical Electric Field Transient at Inner Surface of Shield

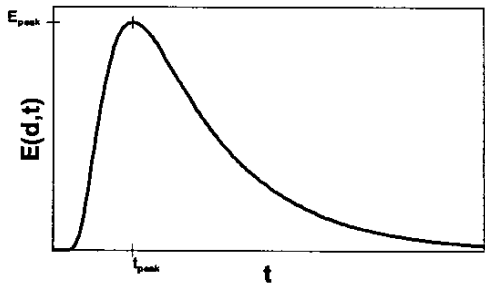


Figure 5. Time variation of typical electric field transient at the inner surface, $E(d,t)$. The peak value of the electric field transient occurs at t_{peak} .

For a purely exponential differential permeability model, it was shown in [2] that for an impulse response, an applied pulse parameter can be defined as

$$\zeta = \frac{Q_0}{\sigma d^2 B_s}$$

where Q_0 is the charge per unit circumference that is transported along the outer surface of the cylinder during the applied pulse. ζ is a fundamental combination of all of the nonmagnetic parameters and the magnetic parameter B_s . The onset of saturation was found to occur at $\zeta=1/2$, in agreement with the limiting nonlinear theory.

COMPUTATIONAL CONSIDERATIONS

Problem Parameters

Differential Permeability

For the calculations considered here, the parameters for the relative differential permeability were

$$B_s = 1.07 \text{ T}$$

$$\mu_{ri} = 8999$$

For these values of B_s and μ_{ri} , it follows from the defining equation for μ_{ri} that

$$H_1 = 94.61928498073560 \text{ amps/m}$$

Electrical Conductivity

The electrical conductivity was

$$\sigma = 6.25 \times 10^6 \text{ siemens / m}$$

Shield Thickness

The shield thickness was

$$d = 1 \times 10^{-4} \text{ m}$$

Applied Pulse

For the applied pulse, the time constants were selected to be much shorter than the transient electric field response so as to be a good approximation to an impulse

$$t_r = 2 \times 10^{-12} \text{ second}$$

$$t_f = 2 \times 10^{-11} \text{ second}$$

For the above time constants, the peak of the applied pulse occurs at approximately

$$t_p = 5.11685576221 \times 10^{-12} \text{ second}$$

at which time the maximum value of the applied pulse is

$$H(0, t_p) = 0.69683731441 A_o \text{ amps / meter}$$

For a given value of the applied pulse amplitude A_o , the applied pulse parameter, ζ , was evaluated using

$$\zeta = \frac{A_o(t_f - t_r)}{\sigma d^2 B_s}$$

For the above problem parameters, the transition to saturation can be expected for

$$A_o = 1.8576388889 \times 10^9 \text{ amps / meter}$$

for which $\zeta = 1/2$.

Computational Approach

Some computational aspects for finite difference time domain (FDTD) solution of the nonlinear problem were considered in [3]. An implicit FDTD formulation with backward time differencing was used.

For the FDTD results considered here, the shield was divided into 500 spatial intervals such that

$$\Delta x = 2 \times 10^{-7} \text{ meter}$$

The calculations were divided into three time sectors:

1. $0 \leq t \leq t_p$ in which 5×10^6 time intervals were used such that

$$\Delta t_1 = 1.02337115244180 \times 10^{-18} \text{ second}$$

2. $t_p \leq t \leq 100t_f$ in which 5×10^7 time intervals were used such that

$$\Delta t_2 = 3.98976628847558 \times 10^{-17} \text{ second}$$

3. $t \geq 100t_f$ in which

$$\Delta t_3 = 1 \times 10^{-12} \text{ second}$$

NUMERICAL RESULTS

To illustrate the results of the numerical investigations, some results are presented for an applied surface pulse with

$$A_o = 1 \times 10^9 \text{ amps / meter}$$

The applied pulse is shown in Figure 6.

$$H(0, t_p) = 6.9683731441 \times 10^8 \text{ amps / meter}$$

for which $\zeta = 0.269155256$. That is, the applied pulse is about 0.5383105127 of that which would be expected to saturate the shield (saturation occurs at $\zeta = 1/2$).

Applied Surface Pulse, $H(0, t)$

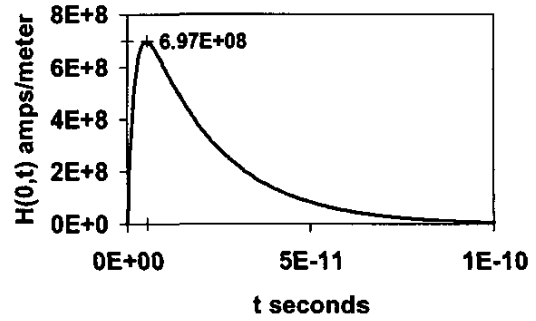


Figure 6. Time variation of the applied surface current pulse $H(0, t)$. The peak value of the applied pulse $H(0, t_p) = 6.97E+8$ amps/meter occurs at $t_p = 5.12E-12$ second.

Finite difference time domain (FDTD) calculations were used to determine the magnetic field intensity, $H(x, t)$, within the shield wall during and after the applied pulse. Selected results are shown in the accompanying figures for four time periods.

H-field from $t=0$ to $t=t_p$

The spatial distributions for selected times up to and including the peak of the applied pulse, t_p , are shown in Figure 7. During this rise time phase of the applied pulse, the H field is being driven into the shield where it is confined to a relatively small portion near the outer surface. Results for selected times up to and including the time of the maximum applied pulse are shown in Figure 7.

H-field Distribution Before Applied Pulse Peak

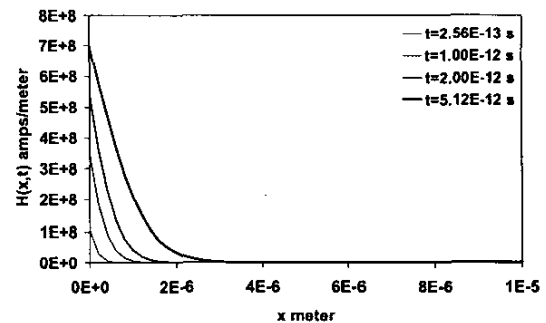


Figure 7. Spatial distribution of $H(x, t)$ at selected times before the peak of the applied surface current pulse $H(0, t)$ at $t_p = 5.12E-12$ second. (Note that figure shows the first 1/10 of the shield from $x=0$ to $x=d/10$.)

of the data reveals that for each time step there is a location at which there is an extremely rapid decrease in H. This

moving transition front separates a region of intense fields from a region of negligible fields. Behind the front the intense fields have driven the shield into saturation; whereas, ahead of the front the small field levels leave the shield essentially unperturbed.

H-field after peak of applied pulse $t=t_p$

The spatial distributions of $H(x,t)$ for selected times at and immediately after the time of the peak of the applied pulse, t_p , are shown in Figure 8. In this fall time phase of the applied pulse, the H field at the surface decreases monotonically from the peak value as the applied pulse decreases exponentially. As the surface pulse decays, the H field near the surface decreases while the H field penetrates deeper into the shield. The front continues to diffuse into the material. Initially, the maximum H field value occurs at the surface of the shield; however, as the applied pulse decreases, there is a time at which the H field at the surface becomes smaller than that inside the shield. For subsequent times the maximum H field value occurs within the shield rather than at the surface. Eventually, the H field at the outer surface becomes vanishingly small such that the H field is essentially zero at the outer surface and at the position of the front.

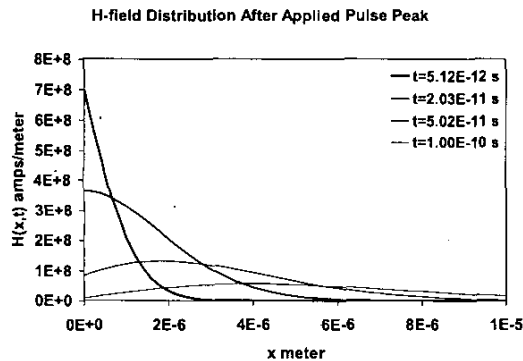


Figure 8. Spatial distributions of $H(x,t)$ at selected times after the peak of the applied surface current pulse $H(0,t)$ at $t_p=5.12E-12$ second. (Note that the figure shows the first part of the shield from $x=0$ to $x=d/10$.)

H-field distribution well after $t=t_p$

Spatial distributions of $H(x,t)$ for selected times well after the applied pulse are shown in Figure 9. At these times, the applied pulse has decayed to a negligible value. The latest time shown is $100t_f=2 \times 10^{-9}$ second, which is the end of the second time sector. In this phase, the H field is no longer being driven by the applied pulse to an appreciable extent (since the applied surface pulse is forced to approach zero exponentially), but continues to diffuse into the shield. The field is now constrained to the inner volume of the shield with amplitude significantly smaller than the peak driving pulse (note finer amplitude scale on plot). Again, the region behind the front is saturated ($\mu_{rd}(H) \approx 1$)

while the region ahead of the front is essentially unsaturated ($\mu_{rd}(H) \approx 9000$).

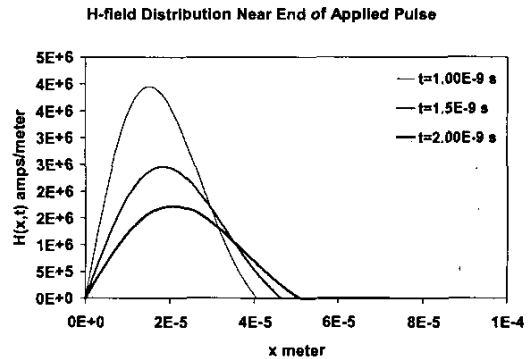


Figure 9. Spatial distributions of $H(x,t)$ at selected times well after the peak of the applied surface current pulse $H(0,t)$ at $t_p=5.12E-12$ second. (Note that the figure shows the full shield from $x=0$ to $x=d$.)

H-field at the time of the peak E-field transient

Eventually the H field will near the inner surface and induce a sizable E field at the inner surface, which is directly proportional to the slope of the H field at the inner surface ($x=d$). As shown in Figure 10, the E field at the inner surface increases with time, passes through a peak value, and then decreased to zero. In the example shown here, the maximum value of the electric field transient occurs at $t_{peak} = 1.28925910000014 \times 10^{-5}$ second and has a value $E_{peak} = 4.67227793813865 \times 10^{-1}$ volts/meter. As can be seen, the maximum value of the electric field transient occurs much later in time (by many orders of magnitude) than the peak value of the applied surface current pulse.

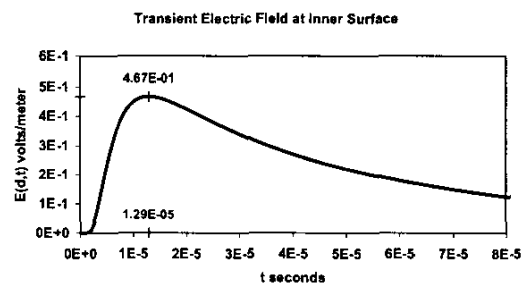


Figure 10. Time variation of the electric field transient at inner surface, $E(d,t)$.

Figure 11 shows the H field distribution at the time of peak electric field transient. The H field is essentially zero at the outer surface ($x=0$) as a result of the decay of the

applied pulse and is constrained to be zero at the inner surface ($x = d$) by the problem formulation.

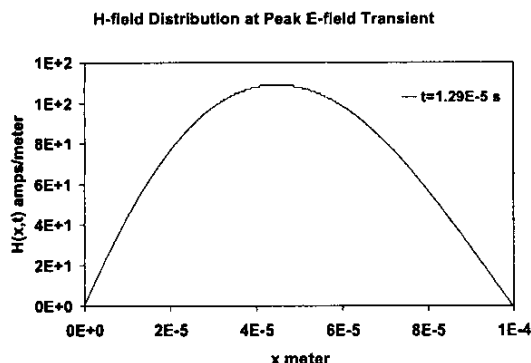


Figure 11. Spatial distribution of $H(x,t)$ at the time of the peak of electric field transient at inner surface $E(d,t)$. (Note that figure shows the full shield from $x=0$ to $x=d$.)

Time for H-field penetration

In order to investigate the propagation of the transition front into the shield, the time at which a prescribed numerical H field value occurred for various spatial gridpoints within the shield was determined. The arbitrary value of $H(x,t) = 1$ amp/meter was chosen as the criterion for the location of the transition front. The times to reach selected gridpoints are shown in Figure 12.

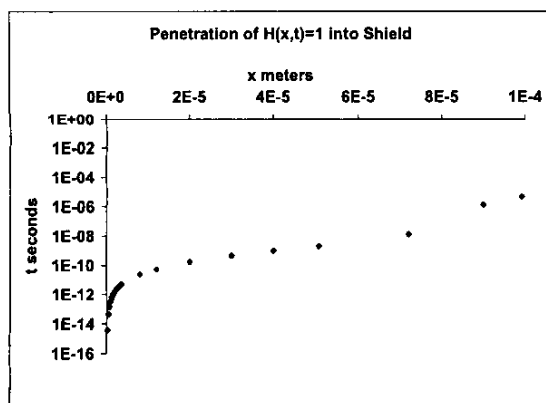


Figure 12. Time for $H(x,t)=1$ amp/meter to penetrate to a prescribed gridpoint.

Initially the transition front propagates very rapidly as the fields are being driven into the shield. After the applied pulse has decayed to a negligible value the transition front slows down considerably. For late times the propagation rate is many orders of magnitude slower than the initial rate.

CONCLUSION

Implicit finite difference time domain (FDTD) calculations were used to determine the magnetic field intensity distribution, $H(x,t)$, within a shield during and after a short

duration double exponential pulse applied to the outer surface. The numerical results show a moving transition front that separates a region of intense fields from a region of negligible fields.

REFERENCES

- [1] William J. Croisant, Carl A. Feickert, and Michael K. McNerney, "A Nonlinear Analytical Procedure for Electromagnetic Transients in Ferromagnetic Shields," 1994 IEEE International Symposium on Electromagnetic Compatibility, August 22-26, 1994, Chicago, IL, Symposium Record 94CH3347-2, pp. 190-195.
- [2] William J. Croisant, Carl A. Feickert, and Michael K. McNerney, "A Nonlinear Analytical Procedure for Electromagnetic Transients in Ferromagnetic Shields with an Exponential Permeability," 1995 IEEE International Symposium on Electromagnetic Compatibility, August 14-18, 1995, Symposium Record 95CH3577-2, pp. 614-619.
- [3] William J. Croisant, Carl A. Feickert, and Michael K. McNerney, "Computational Aspects of a Nonlinear Problem Involving Electromagnetic Transients in Ferromagnetic Shields," 1996 IEEE International Symposium on Electromagnetic Compatibility, August 19-23, 1996, Symposium Record 96CH35906, pp. 424-429.
- [4] William J. Croisant, Carl A. Feickert, and Michael K. McNerney, "An Empirical Correlation for the Calculated Effective Permeability For a Nonlinear Impulse Problem with a Simple Exponential Model for the Relative Differential Permeability" 2002 IEEE International Symposium on Electromagnetic Compatibility, August 19-23, 2002, Symposium Record 02CH37288, Volume 2, pp. 901-906.
- [5] David E. Merewether, "Electromagnetic Pulse Transmission Through a Thin Sheet of Saturable Ferromagnetic Material of Infinite Surface Area," *IEEE Transactions on Electromagnetic Compatibility*, Volume EMC-11, Number 4, November 1969, pp. 139-143.
- [6] Raymond Luebbers, Ken Kumagai, Saburo Adachi, and Toru Uno, "FDTD Calculation of Transient Pulse Propagation through a Nonlinear Magnetic Sheet," *IEEE Transactions on Electromagnetic Compatibility*, Volume 35, February 1993, pp. 90-94.
- [7] Salvatore Celozzi and Marcello D'Amore, "Magnetic Field Attenuation of Nonlinear Shields," *IEEE Transactions on Electromagnetic Compatibility*, Volume 38, Number 3, August 1996, pp. 318-326.
- [8] Giulio Antonini, Saverio Cristina, and Antonio Orlandi, "A Spice Model for Near-Field Transient Analysis of Ferromagnetic Grids," *IEEE Transactions on Electromagnetic Compatibility*, Volume 39, Number 2, May 1997, pp. 114-123.